Available online at www.sciencedirect.com
SCIENCE DIRECT®
Journal of Solid State Chemistry 178 (2005) 2832–2837
JOURNAL OF SOLID STATE CHEMISTRY
www.elsevier.com/locate/jssc

Raman scattering investigations on lanthanum-doped $Bi_4Ti_3O_{12}$–$SrBi_4Ti_4O_{15}$ intergrowth ferroelectrics

Jun Zhu[a,*], Xiao-Bing Chen[a], Jun-Hui He[a], Jian-Cang Shen[b]

[a]College of Physics Science and Technology, Yangzhou University, Yangzhou 225002, China
[b]The National Laboratory of Solid State Microstructures, Nanjing University, Nanjing 210008, China

Received 22 January 2005; received in revised form 13 May 2005; accepted 21 June 2005

Abstract

The ferroelectric ceramics of $Bi_4Ti_3O_{12}$, $SrBi_4Ti_4O_{15}$, and lanthanum-doped $Bi_4Ti_3O_{12}$–$SrBi_4Ti_4O_{15}$ were synthesized, and their Raman spectra were investigated. La-doping resulted in the enlargement of remnant polarization of $Bi_4Ti_3O_{12}$–$SrBi_4Ti_4O_{15}$. The structure of the Bi_2O_2 layers and TiO_6 octahedra of the intergrowth was found to be different from those of $Bi_4Ti_3O_{12}$ and $SrBi_4Ti_4O_{15}$. La^{3+} ions exhibit pronounced selectivity for the occupation of A site as La content is lower than 0.50, and tend to be incorporated into Bi_2O_2 layers when the La content is higher than 0.50. Lanthanum substitution brings about the structural phase transition in $Bi_4Ti_3O_{12}$–$SrBi_4Ti_4O_{15}$. The variation of ferroelectric property may be attributed to combined contribution from the decreasing of the oxygen vacancies, the relaxation of the lattice distortion, the destroying of the insulation and the space charge compensation effects of the Bi_2O_2 slabs.

Keywords: $Bi_4Ti_3O_{12}$–$SrBi_4Ti_4O_{15}$; Lanthanum substitution; Raman spectrum; Ferroelectric property

1. Introduction

Extensive investigations have been paid on ferroelectric thin films due to their potential applications in nonvolatile ferroelectric random access memories (FeRAMs) [1], among which, bismuth layer-structured ferroelectrics (BLSFs) has attracted considerable attentions owing to their promising fatigue-free nature [2]. The crystal structure of BLSFs consists of the interleaved bismuth oxide $(Bi_2O_2)^{2+}$ layers and pseudo-perovskite blocks containing BO_6 octahedra, and its chemical formula is generally expressed as $(Bi_2O_2)^{2+}(A_{m-1}B_mO_{3m+1})^{2-}$. In the above notation, A represents a mono-, bi- or tri-valent ion, B denotes a tetra-, penta- or hexa-valent ion, and m is the number of BO_6 octahedra in each pseudo-perovskite block ($m = 1,2,3, \ldots$) [3]. The BLSFs thin films, such as $SrBi_2Ta_2O_9(m = 2)$ [4], $Bi_4Ti_3O_{12}(m = 3)$ [5], $SrBi_4Ti_4O_{15}(m = 4)$ [6] and $Sr_2Bi_4Ti_5O_{18}(m = 5)$ [7], however, exhibit a relatively low remnant polarization ($2P_r$), which is a major hindrance for their further applications in FeRAMs.

By means of doping, forming an intergrowth, or a solid solution, ferroelectric properties of BLSFs can be improved to a considerable extent [8]. For example, lanthanide substitution for bismuth at the A site, or high-valent cation replacements for titanium at the B site can apparently enhance the $2P_r$ of $Bi_4Ti_3O_{12}$ (BIT) and $SrBi_4Ti_4O_{15}$ (SBTi) [5,9–12]. The $2P_r$ of La-doped BIT and SBTi reaches a maximum value at the La content of 0.75 and 0.25, respectively [9,11]. The enhancement of $2P_r$ is likely related to the decreasing of oxygen vacancies which appears due to inevitable generation of Bi vacancies in BLSFs to meet charge neutrality restrictions [5,11]. Forming intergrowth structure was reported to be another effective way to

*Corresponding author. Fax: +86 514 797 5458.
E-mail addresses: jzhu73@hotmail.com, zhujun@yzu.edu.cn (J. Zhu).

0022-4596/$ - see front matter © 2005 Elsevier Inc. All rights reserved.
doi:10.1016/j.jssc.2005.06.028

enlarge $2P_r$, where the intergrowth ferroelectrics are composed of two BLSFs with different m's [13,14]. For $Bi_4Ti_3O_{12}$–$SrBi_4Ti_4O_{15}$ (BIT–SBTi), its unit cell consists of one from BIT and another from SBTi, and their perovskite blocks in BIT and SBTi are therefore sandwiched between $(Bi_2O_2)^{2+}$ layers as the following sequence: …$(Bi_2O_2)^{2+}$–$(Bi_2Ti_3O_{10})^{2-}$–$(Bi_2O_2)^{2+}$–$(SrBi_2Ti_4O_{13})^{2-}$–$(Bi_2O_2)^{2+}$… [13]. $2P_r$ of BIT–SBTi is enlarged over its two constituents, say, BIT and SBTi. Noguchi et al. reported that this enlargement originates from a quite distinct Bi^{3+} displacement in $(Bi_2O_2)^{2+}$ layers along the a-axis due to the lattice mismatch between two perovskite blocks and their different chemical characters [13,14].

La-doped BIT–SBTi ceramics, $Bi_{4-x}La_xTi_3O_{12}$–$SrBi_{4-y}La_yTi_4O_{15}$ [BLT–SBLT(x+y), $x+y = 0.00\sim 1.50$], are synthesized on the basis of considering both doping and intergrowth effects. It is found that the ferroelectric properties of BIT–SBTi are improved by La-doping. The $2P_r$ reaches a maximum value of 25.6 μC/cm^2 at the La content of 0.50 [15]. In the case of $(x+y) = 0.50$, the La content in BLT and SBLT units is estimated to be 0.29–0.37 and 0.21–0.13, respectively [15,16]. At the maximum value of $2P_r$, the lanthanum content in each unit of BLT–SBLT (0.50) is nearly as same as the La content at which the $2P_r$ maximizes in La-doped SBTi [11,15,16]. To investigate the reason why the $2P_r$ shows the maximum value at the La content of 0.50, Raman scattering is carried out since it is highly sensitive to the local structure and local symmetry, and is a convenient means for structural change observation with a high spatial resolution. The measurement is nondestructive and does not need any special treatments for the samples [17,18]. In this paper, the Raman scattering spectra of BIT, SBTi, and BLT–SBLT at room temperature is investigated to reveal the mechanism of the remnant polarization variation. The Raman scattering spectra of the BIT–SBTi ceramics with the temperature ranging from 20 to 600 °C is presented as well. It is found that as the La content is lower than 0.50, La^{3+} ions only substitute for the Bi^{3+} ions at A site, and they are incorporated into the Bi_2O_2 layers at higher content. Doping brings about the similar structural phase transition to what happens at high temperature.

2. Experiment

The ceramic samples of $Bi_{4-x}La_xTi_3O_{12}$–$SrBi_{4-y}La_yTi_4O_{15}$ [BLT–SBLT(x+y), $x+y = 0.00$, 0.25, 0.50, 0.75, 1.00, 1.25, 1.50], $Bi_4Ti_3O_{12}$, and $SrBi_4Ti_4O_{15}$ are synthesized by the standard solid-state reaction method [19]. Raman scattering spectra are measured in a backward microconfiguration, using the 514.5 nm line from an Ar^+ laser (~300 mW) focused on a spot with a diameter of 1–2 μm on the sample surface. The scattered light is dispersed by a triple spectrometer (Jobin Yvon T64000) and collected with a liquid-nitrogen-cooled charge coupled devices (CCD) detector. To obtain the Raman spectra at different temperatures, the samples are kept in a temperature controlled oven with quartz windows, heated at the rate of 20 °C/min and stabilized at the desired temperature for about 3 min prior to the spectrum measurement.

2.1. Results and discussion

2.1.1. Raman spectra of $Bi_4Ti_3O_{12}$, $Bi_4Ti_3O_{12}$–$SrBi_4Ti_4O_{15}$, and $SrBi_4Ti_4O_{15}$

Fig. 1 shows the Raman spectra of $Bi_4Ti_3O_{12}$, $Bi_4Ti_3O_{12}$–$SrBi_4Ti_4O_{15}$, and $SrBi_4Ti_4O_{15}$ at room temperature. The vibration modes of BLSFs can be classified as internal modes of TiO_6 octahedra and the lattice transition modes related to the motion of the cations in the pseudo-pervoskite slabs and the Bi_2O_2 layers [20]. The modes with the Raman shift lower than 200 cm^{-1} are related to the motion of heavier ions. For the BLSFs, the mode between 50 and 60 cm^{-1} is reported to arise from the displacement of Bi^{3+} ions in Bi_2O_2 layers, while those between 90 and 160 cm^{-1} originate from the vibrations of the ions at the A sites of the pseudo-perovskite blocks. Although Sr^{2+} ion is much lighter than Bi^{3+} (Sr/Bi = 88/209), the radius of Sr^{2+} (0.132 nm) is larger than that of Bi^{3+} (0.117 nm) [21] and the Sr^{2+} ion has a lower chemical valence than that of Bi^{3+} ion. Thus, the mode related to Sr^{2+} ions is expected to locate in the same region as that of Bi^{3+}

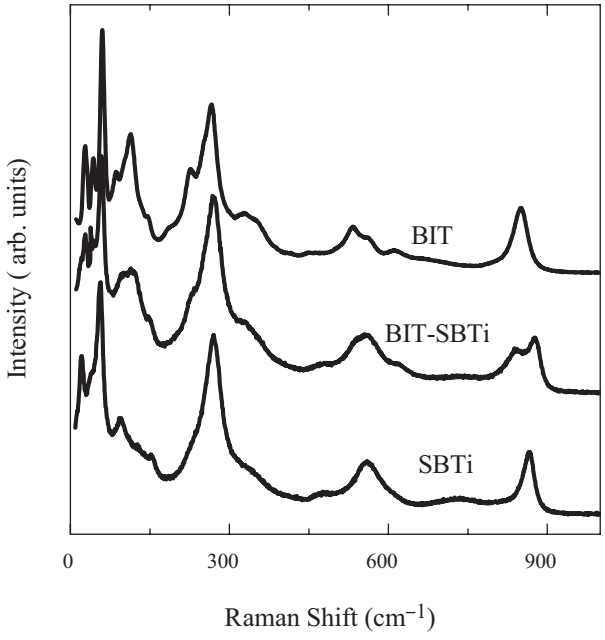

Fig. 1. Raman spectra of $Bi_4Ti_3O_{12}$, $Bi_4Ti_3O_{12}$–$SrBi_4Ti_4O_{15}$, and $SrBi_4Ti_4O_{15}$ at room temperature.

ions [22]. The modes with the Raman shift above 200 cm^{-1} are associated with the TiO_6 octahedra due to the large intragroup binding energy in the octahedra and the much smaller mass of Ti^{4+} ions [20,23]. The mode at ~268 cm^{-1} arises from the torsional bending of TiO_6 octahedra, and those at ~550 and ~850 cm^{-1} correspond to the stretching of TiO_6 [17,18].

The Raman shift of the mode relating to the Bi_2O_2 layers of BIT–SBTi is 58.8 cm^{-1}, which is about the average of BIT (60.4 cm^{-1}) and SBTi (56.5 cm^{-1}). This result implies that the microstructure of Bi_2O_2 layer in the intergrowth is different from that in BIT or SBTi, agreeing with that reported by Noguchi et al [13]. BIT–SBTi exhibits two stretching modes of TiO_6 octahedra located at 839 and 876 cm^{-1}, while the Raman shift for the corresponding modes of BIT and SBTi are 850 and 866 cm^{-1}, respectively. The difference of the frequency of the stretching modes of the TiO_6 octahedra implies that the microstructure of TiO_6 in the BIT–SBTi is different from those in BIT or SBTi, which may contribute to the enlargement of $2P_r$ as well. Besides these two sorts of vibration modes, the other modes for BIT and SBTi can be observed in the spectrum of intergrowth BIT–SBTi without any Raman shift.

2.1.2. *La substitution sites in La-doped* $Bi_4Ti_3O_{12}-SrBi_4Ti_4O_{15}$

La^{3+} ions can substitute for Bi^{3+} ions in $(Bi_2O_2)^{2+}$ layers and in pseudo-perovskite blocks, since the chemical valence of La^{3+} is the same as that of Bi^{3+} and their ion radii are almost identical (La^{3+}: 1.160 Å, Bi^{3+}: 1.170 Å) [21]. The atomic site in BLT–SBLT where La substitute for can be determined according to the Raman modes relating to vibrations of the Bi^{3+} ions in the Bi_2O_2 layers and at the A sites of the pseudo-perovskite blocks. Fig. 2 shows the Raman spectra of La-doped BIT–SBTi intergrowth ferroelectrics with the La content ranging from 0.00 to 1.50. To clarify the movements of the modes with low frequencies, the modes with the Raman shift lower than 200 cm^{-1} for different La content are presented in Fig. 3. Fig. 4(a)–(d) illustrates the Raman shift change of the modes at 58.8, 100.3, 117.4, and 146.0 cm^{-1} upon La content. It can be seen that the modes at 58.8 and 100.3 cm^{-1} apparently shift to lower frequency with La-doping, while those at 117.4 and 146.0 cm^{-1} move to higher frequency. Moreover, the intensity of these modes with lower frequencies decreases with La-doping.

For the case of $(x+y)\leqslant 0.50$, the Raman shift of the modes at 58.8 cm^{-1} corresponding to the vibration of Bi^{3+} ions in the Bi_2O_2 layers does not change with La-doping. This implies that La^{3+} ions are almost not incorporated into the Bi_2O_2 layers. With the further La-doping, the Raman shift decreases from 58.8 to 55.0 cm^{-1}, which is possible due to the La^{3+} substitution for the Bi^{3+} in Bi_2O_2 slabs. This result agrees well with

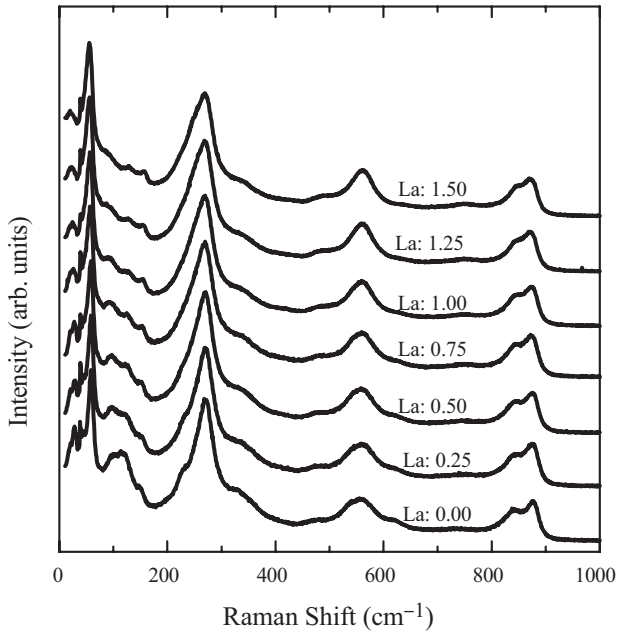

Fig. 2. Raman spectra of BLT–SBLT(x+y) with the Raman shift ranging from 8 to 1000 cm^{-1} at room temperature.

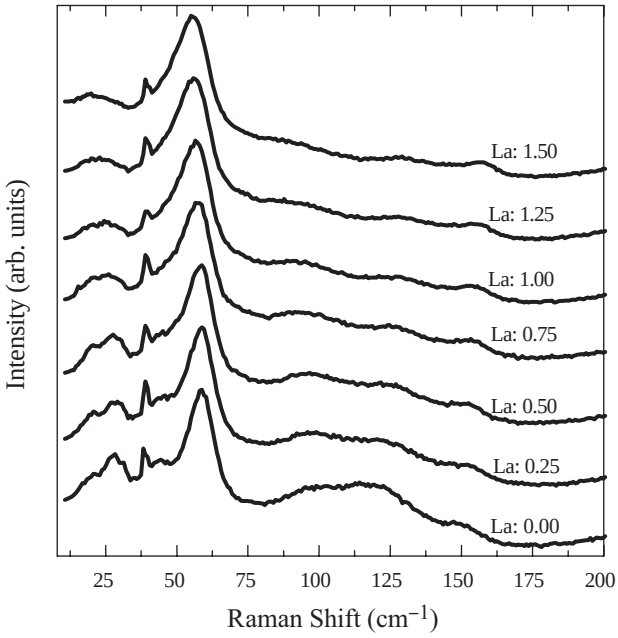

Fig. 3. Raman spectra of BLT–SBLT(x+y) with the Raman shift lower than 200 cm^{-1} at room temperature.

the shifts of Raman modes at 100.3, 117.4, and 146.0 cm^{-1}, which correspond to the vibration of the ions at A sites of the pseudo-perovskite blocks. Compared to the case of $(x+y)>0.50$, these three modes shift more significantly in the case of $(x+y)\leqslant 0.50$, which implies that the influence of doping on the pseudo-perovskite blocks is weaker in the former case. Since no La^{3+} ions are incorporated into the Bi_2O_2

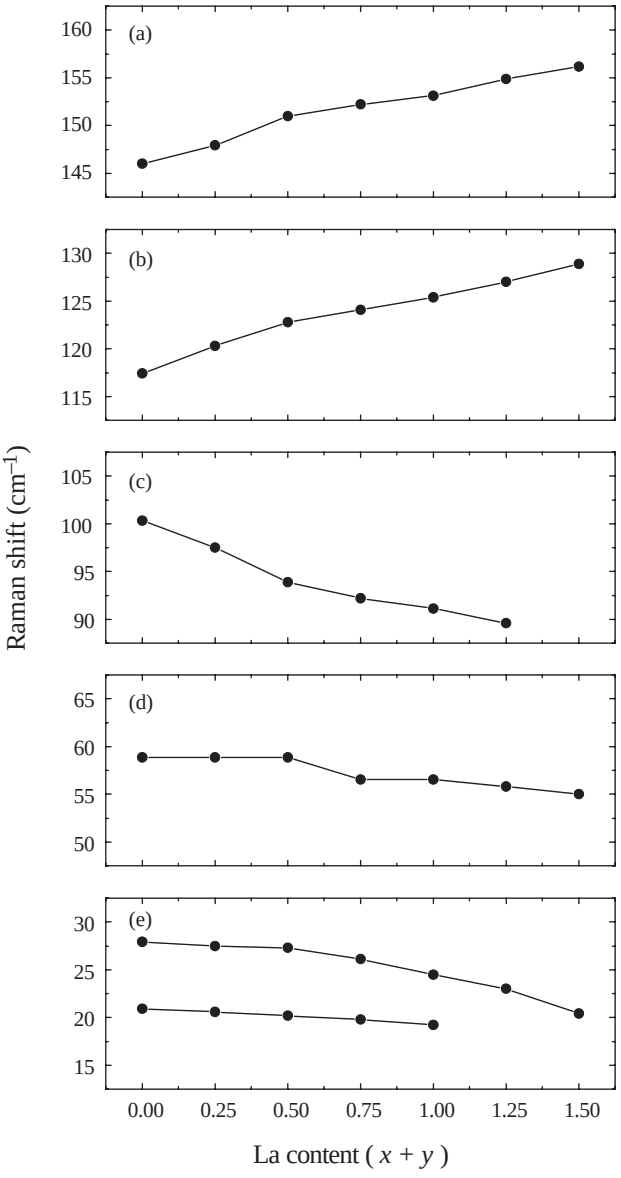

Fig. 4. Dependences of the Raman shifts lower than 200 cm^{-1} for BLT–SBLT(x+y) on the La content.

slabs as $(x+y)\leqslant 0.50$, all of La^{3+}/Bi^{3+} substitution occurs exclusively at A site of pseudo-pervoskite blocks. When the La content higher than 0.50, La^{3+}/Bi^{3+} substitution occurs not only at the A site, but also in the Bi_2O_2 slabs. Thus, the La-substitution sites in BLT–SBLT can be concluded. When La content less than 0.50, La^{3+} ions prefer to occupy the A site of the pseudo-perovskite blocks. While La content higher than 0.50, some La^{3+} ions tend to be incorporated in to Bi_2O_2 layers.

The previous investigations [20] on the lanthanum-doped $Bi_4Ti_3O_{12}$ revealed that La^{3+} ions start to substitute for the Bi^{3+} in Bi_2O_2 layers as the La content reaches 1.00. The studies on the La-doped $SrBi_4Ti_4O_{15}$ suggested that La^{3+} ions are incorporated into the Bi_2O_2 layers with La content between 0.10 and 0.25 [22]. Based on the relationships of the Curie temperature or the lattice space for the BLT–SBLT intergrowth ferroelectrics and its constituents, BLT and SBLT, the La distribution in La-doped BIT–SBTi has been calculated. As for BLT–SBLT(0.50), the La content is 0.29–0.37 in BLT unit and 0.21–0.13 in SBLT unit, respectively [15,16]. As the La^{3+} ions start to substitute for the Bi^{3+} in the Bi_2O_2 layers, the La content in SBLT unit of BLT–SBLT is close to that in La-doped SBTi. This interesting phenomenon probably originates from the special structure of the intergrowth ferroelectrics. In BIT–SBTi, the $(Bi_2O_2)^{2+}$ slabs locate between the pseudo-perovskite blocks of BIT and SBTi units, $(Bi_2Ti_3O_{10})^{2-}$ and $(SrBi_2Ti_4O_{13})^{2-}$ blocks, alone the c axis [13]. As the La-doping content is 0.50, the actual La distribution in the SBLT units reaches 0.13–0.21, which is the critical value for La^{3+} ion acceptability of the pseudo-perovskite blocks of the SBTi units. Then the La^{3+} ions are incorporated into the $(Bi_2O_2)^{2+}$ slabs through the side of $(SrBi_2Ti_4O_{13})^{2-}$ slabs.

The substitution of light La^{3+} for heavy Bi^{3+} ions (La/Bi = 139/209) leads to the higher frequency of the phonon mode. On the other hand, La^{3+} ions substitution may lower the corresponding binding strength and decrease the Raman shift due to the lower binding energy of La 4d (~102 eV) in comparison with that of Bi 4f (~163 eV) [22]. The combined effects of the binding strength and the ion mass result in the change of Raman shift. As $(x+y)>0.50$, the decreasing of the mode at 58.8 cm^{-1} implies that the influence of doping on the binding strength is more significant than that on the mass. Not only the bond connecting the replaced ions, but also the bonds related to the other unsubstituted ions vary with doping significantly. The hardening of the modes at 117.4 and 146.0 cm^{-1} corresponding to the vibration of the Bi ions at A site is related to the dominating influence of the lighter La^{3+} substitution for the heavier Bi^{3+} ions. However, the mode at 100.3 cm^{-1} due to the vibration of ions at A sites moves to the lower frequency with La-doping. This is similar to the change of the corresponding mode in La-doped in $SrBi_4Ti_4O_{15}$ and is different from the mode in La-doped $Bi_4Ti_3O_{12}$. In BLT-x, all the modes related to the vibration of the ions at A sites increase with La-doping [20]. While in SBLT, the mode for the Sr^{2+} ion at A site decreases with doping, since the Sr^{2+} ion is not substituted by La^{3+} and the incorporation of La^{3+} ions into the pseudo-perovskite slabs lowers the binding strength [22]. Thus, the mode at 100.3 cm^{-1} in BIT–SBTi is due to the Sr^{2+} ion at the A site of SBTi unit, and it moves to lower frequency with La-doping.

The mode at ~268 cm^{-1} from the torsional bending of TiO_6 octahedra does not shift with doping. However, lanthanum-doping results in the movement of the modes corresponding to the stretching vibration of TiO_6 octahedra. In the spectrum of BIT–SBTi, the mode at

$\sim$550 cm^{-1} is broad and seems to be composed of two Raman modes at $\sim$540 and $\sim$560 cm^{-1}. Upon La-doping, the mode at $\sim$540 cm^{-1} moves toward higher frequency and is overlapped with the mode at $\sim$560 cm^{-1}. As the La content is higher than 1.00, the modes with lower frequency is not detectable. Meanwhile, the stretching modes at $\sim$839 and $\sim$876 cm^{-1} move towards each other with La-doping. The movements of the stretching modes indicate that the structural difference of TiO_6 octahedra between BLT and SBLT units tend to disappear with doping.

2.1.3. Soft modes and structural phase transition

Displacive ferroelectrics normally have at least one low-energy mode which corresponding to the vibration of the ions at *A* site with respect to the chains of TiO_6 octahedra [20]. When Curie temperature (T_c) is approaching, the low-energy mode softens. This can be observed in the spectra of BIT and SBTi [23]. The studies on La-doped BIT and SBTi indicate that substitution brings about the similar softening of the low-frequency modes at room temperature. And the structural phase transition can be achieved by the compositional modifications [20,22].

$Bi_4Ti_3O_{12}$–$SrBi_4Ti_4O_{15}$ is a type of displacive ferroelectric material as well. In its Raman spectrum there are two soft modes with the Raman shifts at about 28 and 21 cm^{-1}, respectively. When the La content increases from 0.00 to 1.50, the two modes shift towards lower frequency accompanying with the decrease of intensity, as indicated in Fig. 3. The Raman shifts of the soft modes as functions of La content are shown in Fig. 4(e). The mode at about 28 cm^{-1} for BIT–SBTi shifts significantly with the increasing La content. The mode at 21 cm^{-1} moves slowly. And it cannot be detected at high La-content, which may be due to the decrease of its intensity and overlapping with the soft mode at 28 cm^{-1}. The temperature dependence of the Raman scattering spectra of $Bi_4Ti_3O_{12}$–$SrBi_4Ti_4O_{15}$ is shown in Fig. 5. Because the scattered light transfers through the quartz windows of the temperature controlling oven, the intensities of Raman spectra are weakened. It is clear, however, that all of the modes exhibit a remarkable softening with the increase of the measuring temperature. The intensities of the modes decreases and the Raman modes shift towards lower frequencies as the temperature increases from room temperature to 600 °C. The two modes at 21 and 28 cm^{-1} soften upon heating, and disappear at about 100 °C below the Curie temperature, which is similar to the lowest mode in the $SrBi_2Ta_2O_9$ [24]. The similar softening behavior of the modes at 21 and 28 cm^{-1} upon doping and heating suggests that lanthanum substitution brings about the structural phase transition in BIT–SBTi intergrowth ferroelectric material.

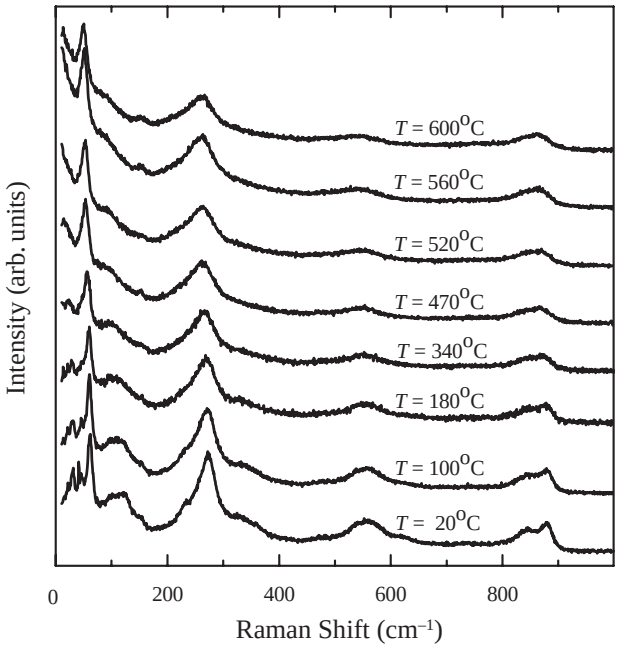

Fig. 5. Raman spectra of $Bi_4Ti_3O_{12}$–$SrBi_4Ti_4O_{15}$ at the temperature ranging from 20 to 600 °C.

2.1.4. Origination of remnant polarization variation

In the un-doped BLSFs, the ions at *A* site strongly deviate from the ideal center of the perovskite structure, leading to the lattice distortion [20]. As the sample is heated up, or the nonpolarizable La^{3+} ions substitute for Bi^{3+}, the ions at *A* site move towards the ideal center of the perovskite structure, and reduces the lattice distortion. This phenomenon is consistent with the softening of the low-frequency modes [20,22]. The displacement of the ions at *A* site of perovskite blocks is the major origination of the spontaneous polarization [20]. Therefore, La-doping brings about the decrease of the spontaneous polarization in BIT–SBTi.

A number of oxygen vacancies in BIT–SBTi will be generated with the inevitable bismuth vacancies under charge neutrality restrictions. The oxygen vacancies act as space charge, causing strong domain pinning and reducing remnant polarization, as has been proved in the $Pb(Zr,Ti)O_3$ thin films [25,26]. Theoretical calculations also suggested that the increase in defect concentration leads to a decrease of remnant polarization [27]. When the more stable La replaces the volatile Bi, the generation of oxygen vacancies is restrained, and in turn enlarges the remnant polarization. On the other hand, La-doping also brings about the decrease in spontaneous polarization, as mentioned above. With low La content, the effect of the oxygen vacancy restraint is dominant, so the remnant polarization is enhanced. For BLSFs, it is widely accepted that the $(Bi_2O_2)^{2+}$ layers exert very important influence on the electric properties: the Bi_2O_2 layers act as the insulated layers and are self regular to compensate for space charge due to their net

electric charge [4,28]. In our case, when the La content is higher than 0.50, the La^{3+} ions are incorporated into Bi_2O_2 layers, which destroys the original effects of the insulated layers and the space charge compensation, decreasing the remnant polarization. It means that the incorporation of La^{3+} ions into the Bi_2O_2 layers gives an additional effect which decreases the $2P_r$. This negative effect on the polarization, combined with the relaxation of the lattice distortion, weakens the positive effect from the restraint of the oxygen vacancies. Therefore, in La-doped $Bi_4Ti_3O_{12}$–$SrBi_4Ti_4O_{15}$ intergrowth ceramics, the $2P_r$ maximizes at the La content of 0.50, then decreases with doping.

3. Conclusions

The Raman spectra of La-doped $Bi_4Ti_3O_{12}$–$SrBi_4Ti_4O_{15}$ ceramics suggest that La^{3+} ions demonstrate a pronounced site selectivity for the *A* site of the pseudo-perovskite blocks as the La content is lower than 0.50. La^{3+} ions are incorporated into the Bi_2O_2 layers when the La content higher than 0.50. La-doping brings about the structural phase transition in BIT–SBTi. Substitution results in the restraint of the oxygen vacancies, the relaxation of the lattice distortion, and the destroying of the effects of the insulated layers and the space charge compensation of the Bi_2O_2 slabs. These three mechanisms give birth to the variation of the ferroelectric property in La-doped $Bi_4Ti_3O_{12}$–$SrBi_4Ti_4O_{15}$ intergrowth ferroelectric material.

Acknowledgments

The authors gratefully thank Dr. Qing-Ming Zhang for helpful discussions and acknowledge the financial support from the National Natural Science Foundation of China (Grant no. 10274066) and the Natural Science Foundation of Education Bureau of Jiangsu Province, China (Grant no. GK0410181).

References

[1] U. Chon, H.M. Jang, M.G. Kim, C.H. Chang, Phys. Rev. Lett. 89 (2002) 87601.
[2] J.K. Lee, C.H. Kim, H.S. Suh, K.S. Hong, Appl. Phys. Lett. 80 (2002) 3593.
[3] H. Irie, M. Miyayama, T. Kudo, J. Appl. Phys. 90 (2001) 4089.
[4] C. A-Paz de Araujo, J.D. Cuchiaro, L.D. McMillan, M.C. Scott, J.F. Scott, Nature (London) 374 (1995) 627.
[5] B.H. Park, B.S. Kang, S.D. Bu, T.W. Noh, J. Lee, W. Jo, Nature (London) 401 (1999) 683.
[6] S.T. Zhang, B. Yang, Y.F. Chen, Z.G. Liu, X.B. Yin, Y. Wang, M. Wang, N.B. Ming, J. Appl. Phys. 91 (2002) 3160.
[7] S.T. Zhang, C.S. Xiao, A.A. Fang, B. Yang, B. Sun, Y.F. Chen, Z.G. Liu, N.B. Ming, Appl. Phys. Lett. 76 (2000) 3112.
[8] J.S. Zhu, D. Su, X.M. Lu, H.X. Qin, Y.N. Wang, D.Y. Wang, H.L.W. Chan, K.H. Wong, C.L. Choy, J. Appl. Phys. 92 (2002) 5420.
[9] T. Takenaka, K. Sakata, Ferroelectrics 38 (1981) 769.
[10] Y. Noguchi, M. Miyayama, Appl. Phys. Lett. 78 (2001) 1903.
[11] J. Zhu, W.P. Lu, X.Y. Mao, R. Hui, X.B. Chen, Jpn. J. Appl. Phys. (Part 1) 42 (2003) 5165.
[12] J. Zhu, X.Y. Mao, X.B. Chen, Solid State Commun. 129 (2004) 707.
[13] Y. Noguchi, M. Miyayama, T. Kudo, Appl. Phys. Lett. 77 (2000) 3639.
[14] M. Noda, T. Nakaiso, K. Takarabe, K. Kodama, M. Okuyama, J. Cryst. Growth 237 (2002) 478.
[15] J. Zhu, X.B. Chen, W.P. Lu, X.Y. Mao, R. Hui, Appl. Phys. Lett. 83 (2003) 1818.
[16] J. Zhu, X.Y. Mao, X.B. Chen, J. Cryst. Growth. 277 (2005) 462.
[17] N. Sugita, E. Tokumitsu, M. Osada, M. Kakihana, Jpn. J. Appl. Phys. (Part 2) 42 (2003) L944.
[18] N. Sugita, M. Osada, E. Tokumitsu, Jpn. J. Appl. Phys. (Part 1) 40 (2002) 6810.
[19] J. Zhu, R. Hui, X.Y. Mao, W.P. Lu, X.B. Chen, Z.P. Zhang, J. Appl. Phys. 94 (2003) 5143.
[20] M. Osada, M. Tada, M. Kakihana, T. Watanabe, H. Funakubo, Jpn. J. Appl. Phys. (Part 1) 40 (2001) 5572.
[21] R.D. Shannon, Acta. Cryst. A 32 (1976) 751.
[22] J. Zhu, X.B. Chen, Z.P. Zhang, J.C. Shen, Acta. Mater. 53 (2005) 3155.
[23] S. Kojima, R. Imaizumi, S. Hamazaki, M. Takashige, Jpn. J. Appl. Phys. (Part 1) 33 (1994) 5559.
[24] S. Kojima, I. Saitoh, Physica B 263–264 (1999) 653.
[25] Y. Noguchi, I. Miwa, Y. Goshima, M. Miyayama, Jpn. J. Appl. Phys. (Part 2) 39 (2000) L1259.
[26] T. Friessnegg, S. Aggarwal, R. Ramesh, B. Nielsen, E.H. Poindexter, D.J. Keeble, Appl. Phys. Lett. 77 (2000) 127.
[27] L. Baudry, J. Appl. Phys. 86 (1999) 1096.
[28] S.K. Kim, M. Miyayama, H. Yanagida, Mater. Res. Bull. 31 (1996) 121.